Received: 17 August 2023 | Revised: 19 February 2024 | Accepted: 20 February 2024

DOI: 10.1002/pmic.202300312

Proteomics
Proteomics and Systems Biology

RESEARCH ARTICLE

Varroa destructor parasitism and Deformed wing virus infection in honey bees are linked to peroxisome-induced pathways

Tomas Erban[1] | **Dominika Kadleckova**[2] | **Bruno Sopko**[1] | **Karel Harant**[3] | **Pavel Talacko**[3] | **Martin Markovic**[1] | **Martina Salakova**[2] | **Klara Kadlikova**[1] | **Ruth Tachezy**[2] | **Jan Tachezy**[4]

[1]Proteomics and Metabolomics Laboratory, Crop Research Institute, Prague 6-Ruzyne, Czechia

[2]Department of Genetics and Microbiology, Faculty of Science BIOCEV, Charles University, Vestec, Czechia

[3]Proteomics Core Facility, Faculty of Science BIOCEV, Charles University, Vestec, Czechia

[4]Department of Parasitology, Faculty of Science BIOCEV, Charles University, Vestec, Czechia

Correspondence
Tomas Erban, Proteomics and Metabolomics Laboratory, Crop Research Institute, Drnovska 507/73, Prague 6-Ruzyne, CZ-16106, Czechia.
Email: erban@vurv.cz
arachnid@centrum.cz

Funding information
Ministry of Agriculture of the Czech Republic, Grant/Award Numbers: QK1910018, RO0423; Charles University, Grant/Award Number: SVV260679; European Regional Development Fund (ERDF) project CePaViP, Grant/Award Number: CZ.02.1.01/0.0/0.0/16_019/0000759

Abstract

The ectoparasitic mite *Varroa destructor* transmits and triggers viral infections that have deleterious effects on honey bee colonies worldwide. We performed a manipulative experiment in which worker bees collected at emergence were exposed to *Varroa* for 72 h, and their proteomes were compared with those of untreated control bees. Label-free quantitative proteomics identified 77 differentially expressed *A. mellifera* proteins (DEPs). In addition, viral proteins were identified by orthogonal analysis, and most importantly, Deformed wing virus (DWV) was found at high levels/intensity in *Varroa*-exposed bees. Pathway enrichment analysis suggested that the main pathways affected included peroxisomal metabolism, cyto-/exoskeleton reorganization, and cuticular proteins. Detailed examination of individual DEPs revealed that additional changes in DEPs were associated with peroxisomal function. In addition, the proteome data support the importance of TGF-β signaling in *Varroa*–DWV interaction and the involvement of the mTORC1 and Hippo pathways. These results suggest that the effect of DWV on bees associated with *Varroa* feeding results in aberrant autophagy. In particular, autophagy is selectively modulated by peroxisomes, to which the observed proteome changes strongly corresponded. This study complements previous research with different study designs and suggests the importance of the peroxisome, which plays a key role in viral infections.

KEYWORDS
Apis mellifera, autophagy, DWV, host-pathogen interaction, lipid metabolism

Abbreviations: 2D-E-MS/MS, 2D electrophoresistandem mass spectrometry; AFV, Apis flavivirus; A. mellifera, Apis mellifera; AmFV, Apis mellifera filamentous virus; BlastP, protein-protein BLAST; BMLV, Bee macula-like virus; BQCV, Black queen cell virus; CCD, Conserved Domains Database; CoA, coenzyme A; CRI, Crop Research Institute; DEPs, differentially expressed A. mellifera proteins; DOI, digital object identifier; DWV, Deformed wing virus; ER, endoplasmic reticulum; FDR, false discovery rate; IMD, immune deficiency; JAK/STAT, Janus kinases (JAKs) / signal transducer and activator of transcription proteins (STATs); KBV, Kashmir bee virus; KEGG, Kyoto Encyclopedia of Genes and Genomes; LFQ, label-free quantitative; MassIVE, Mass Spectrometry Interactive Virtual Environment; MMTS, methanethiosulfonate; MOB1, MOB kinase activator-like 1; MS, mass spectrometry; MS/MS, tandem mass spectrometry; mTOR, mammalian target of rapamycin; MZE, Ministry of Agriculture of the Czech Republic; nanoLC, nanoliquid chromatography; NAZV, National Agency for Agricultural Research of the Ministry of Agriculture of the Czech Republic; NCBI, National Center for Biotechnology Information; NetoVIR, Novel Enrichment Technique of Viromes; NF-?B, nuclear factor kappa-light-chain-enhancer of activated B cells; PBS, phosphate-buffered saline; PCA, principal component analysis; PPO, prophenoloxidase; Prx5, peroxiredoxin-5; Romo1, reactive oxygen species modulator 1; qPCR, quantitative polymerase chain reaction; RefSeq, Reference Sequence; RNA, ribonucleic acid; ROS, reactive oxygen species; SBV, Sacbrood virus; SDC, sodium deoxycholate; TCEP, Tris(2-carboxyethyl) phosphine hydrochloride; TLR4, Toll-like receptor 4; Tmed7, transmembrane emp24 domain-containing protein 7; TGF-β, transforming growth factor β; V. destructor, Varroa destructor.

1 | INTRODUCTION

The invasive ectoparasitic mite *Varroa destructor* (Anderson & Trueman, 2000) is currently distributed worldwide [1, 2], including in Australia, where the first outbreak was recorded in 2022 [3, 4]. The mite has become a major threat to honey bees since it shifted and broadened in the 1950s from the eastern honey bee *Apis cerana* Fabricius, 1793, to the western honey bee *Apis mellifera* Linnaeus, 1758. The infestation of honey bee colonies by *Varroa* is connected to virus transmission and an increase in viral load [5, 6]. *Varroa* infestation is closely associated with Deformed wing virus (DWV), which is a cause of bee deformation and is considered the most common sign of varroosis worldwide [2]. Moreover, DWV infection is driven by the spread of *Varroa* mite populations throughout the world [7]. Notably, a virome analysis of bee populations in central Europe and the subsequent comparison of this population with naive Australian bee populations, which were free of both *Varroa* and DWV at the time of the study, indicated that DWV profoundly affects the composition of the virome in the new host [8, 9]. Thus, the *Varroa*–DWV interaction is profound and affects the survival and function of bee colonies. Understanding the mechanisms of interaction among mites, viruses, and honey bees is important for the implementation of strategies to prevent the weakening and death of bee colonies.

The negative effect of mite parasitism is connected to the weakening of the host, as the parasite consumes nutrients, resulting in lower protein and carbohydrate levels in bees [10]. Using a proteomic approach, *Varroa* bodies were shown to carry numerous proteins acquired from host honey bees [11, 12], and viral proteins have also been identified in these mites [11]. Additionally, cell components such as those from the fat body [13] together with hemolymph components have been identified in mites [11]. 2D electrophoresis–tandem mass spectrometry (2D-E-MS/MS) proteomic analysis of 1-day-old bee hemolymph revealed the effect of *Varroa* on diverse physiological processes, such as energy metabolism, detoxification, the oxidative stress response, and olfaction [14].

The effect of *Varroa* parasitism and DWV infection on the immune response of bees is controversial. An increase in the DWV load mediated by *Varroa* was associated with the suppression of immunity-related markers (e.g., antimicrobial peptides and enzymes) due to *Varroa* parasite in capped comb cells [15, 16]. Studies on *Varroa*-parasitized larvae have indicated that the negative effect of DWV on humoral and cellular immune responses is mediated through NF-κB signaling, as indicated by the observation of dorsal-1A, Amel\LRR, and apidaecin expression [16, 17]. A quantitative proteomic analysis of emerging bees suggested that *Varroa* infection disrupts host autophagy via modulation of TGF-β signaling. In addition, the synergistic effects of *Varroa* and DWV modulate NF-κB and JAK/STAT signaling, both of which are associated with autophagy [18]. However, in other studies, only a weak association between *Varroa* infection and immunosuppression was observed [19–21]. Most recently, a significant upregulation of the immune response of bees to *Varroa* infection was observed in 10-day-old bees from *Varroa*-infested colonies compared with those from control colonies [22]. Specifically, the antimicrobial peptides apidaecin, abaecin, defensin, and hymenoptaecin were strongly upregulated in *Varroa*-parasitized bees. Conversely, the expression of the NF-κB-like *Relish* gene, which induces a humoral response (in the IMD pathway), was downregulated [22]. The observed differences in the impact of *Varroa* mites on bees reported in various studies most likely resulted from differences in experimental designs and the use of different developmental stages and castes of bees [23, 24].

Significance statement

Varroa destructor is the greatest threat to honey bees worldwide. The disease caused by mites is called varroosis and is associated with the appearance of crippled bees and leads to weakened colonies. It is known that *Varroa* parasitism triggers DWV infection, while in the absence of a mite, the virus can reach a persistent state. To date, different studies have produced different results regarding the effect of *Varroa*–DWV interaction on honey bees. This variation is caused by differences in developmental stages and study designs. We designed a manipulative experiment to study the *Varroa*–DWV interaction. This study is the first to report the effect of *Varroa* on the proteome of 3-day-old worker bees exposed to high *Varroa* loads after emergence. Using high-throughput proteomic analysis, we identified significant changes in *Varroa*-treated and control bees, suggesting the importance of the role of peroxisomes. Until now, the role of peroxisomes in *Varroa*–DWV interactions has not been emphasized, although peroxisomes play a crucial role in viral infections. In addition, we complemented the previously suggested role of the TGF-β signaling pathway in *Varroa* parasitism.

In this study, we exposed previously unparasitized emerged worker bees for 3 days (72 h) to *Varroa* mites collected from a collapsing diseased bee colony with typical symptoms of varroosis. Using label-free quantitative proteomics, we observed proteomic changes in honey bees after exposure to the mites, and from the same data, we retrieved information about the viruses present in the experimental bees. We analyzed the key pathways involved and compared the changes with those found in previous studies that investigated *Varroa*–virus exposure.

2 | MATERIALS AND METHODS

2.1 | Approach and samples

All the biological samples were collected in mid-July, when *Varroa* infestations are generally very infrequent and collapsing colonies are exceptional. The experimental scheme, including an overview of the analyses, is shown in Figure 1.

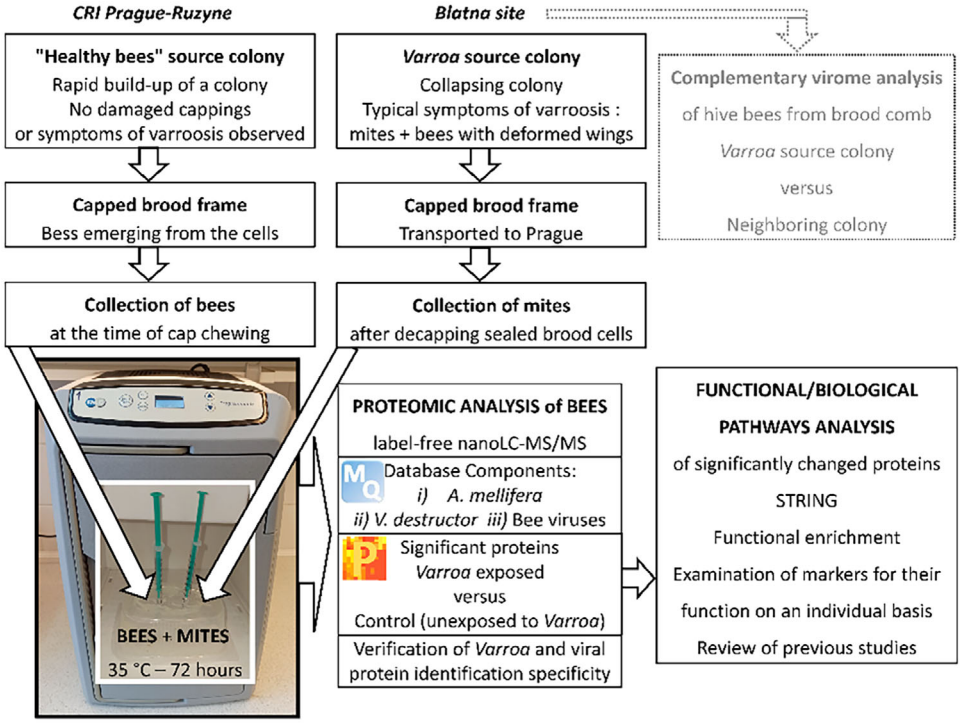

FIGURE 1 The overall approach used in this study.

2.1.1 | Unparasitized emerging *Apis mellifera* worker bees

The bees used for the manipulative experiment originated from a colony at the Crop Research Institute (CRI), Prague. The worker bees were collected from a brood frame at the time of emergence when they were chewing the cell cap [18, 25, 26]. The experimental bees had no obvious defects, were vital, and had no mites found on them or in their cells when they were collected. In addition, the colony had a rapid buildup with no damaged cappings, and no obvious symptoms of bee diseases were observed in the colony throughout the season.

2.1.2 | Varroa destructor

The mites came from a collapsing colony with typical symptoms of varroosis, located at another site about 100 km away from CRI in the South Bohemian municipality of Blatna, Czechia. On July 12, a frame with a sealed brood was taken from the diseased colony and transported to the laboratory in Prague, where the female mites were collected after the comb caps were disturbed by circular motion using a toothpick.

2.1.3 | The manipulative experiment

The emergent bees were placed in plastic chambers with mesh lids on the bottom. The chambers were equipped with two 1-mL syringes placed at the top of the chamber to provide a feed consisting of a 50% (w/v) sugar solution prepared by dissolving granulated beet sugar. The experiment was started by placing 50 mites on 11 worker bees with a brush in a chamber through the opening of the syringe. The same number of bees were placed in a different chamber without mites. Both chambers were incubated in a portable ICT-P mini-incubator (FALC Instruments, Treviglio, Italy) of 18 L in volume (internal dimensions 275 × 185 × 335 mm) with circulating air, a precision of ± 0.2°C and a stability of ± 0.2°C. The exposure lasted for 72 h at 35°C. The availability of the sugar feed supply in the syringes was continuously checked. At the end of the exposure period, the bees were collected, and mites were removed with a brush. The bees were placed in 0.5 mL microvials and immediately frozen on dry ice (~ −70°C). Samples were then stored in a deep freezer at −80°C until analysis. At the end of the experiment, the number of dead and live mites were counted.

2.1.4 | Use of bees for virome analysis

At the Blatna site, additional samples were collected from the *Varroa* source colony and a neighboring colony. The samples included bees that were shaken from the brood frame into a plastic bag and then frozen on dry ice. Later, the samples were stored at −80°C and used for analysis of the bee virome, which provided complementary data to the manipulative experiment.

2.2 | Proteomic analysis of bees

Ten control and ten *Varroa*-exposed bees from the manipulative experiment were subjected to label-free quantitative (LFQ) mass

spectrometry (MS) analysis. Each bee was homogenized in 2.5 mL of homogenization buffer consisting of 100 mM triethylammonium bicarbonate buffer (TEAB; Cat No. 90360; Sigma–Aldrich) and 2% sodium deoxycholate (SDC; Cat No. 30970, BioXtra, Sigma–Aldrich) in a 5-mL glass Potter–Elvehjem tissue grinder (Kartell Labware division, Noviglio, Italy) with a Teflon pestle operated by a drill. The homogenization was completed on ice in three cycles, with each cycle involving 1 min of homogenization followed by incubation on ice for 10 min. The homogenate was transferred to a 15-mL centrifugation tube and centrifuged for 10 min at 3000 × g at 4°C in an MR 23i centrifuge (Jouan Industries, France). The supernatant was collected, divided into aliquots, and stored at −80°C until analysis. Further sample processing and MS analysis were performed as previously described [27]. Briefly, the protein concentration was determined using a BCA protein assay kit (Cat No. 23225, Thermo Fisher Scientific, MA, USA). Cysteines were reduced with Tris(2-carboxyethyl) phosphine hydrochloride (TCEP) and blocked with methyl methanethiosulfonate (MMTS). The samples were digested with porcine trypsin. Then, the samples were acidified with trifluoroacetic acid to a final concentration of 1%. SDC was removed by extraction to ethylacetate and subsequently to hexane. Peptides were desalted using a Michrom C18 column. The dried peptides were resuspended in 25 µL of water containing 2% acetonitrile and 0.1% trifluoroacetic acid. The samples were injected into the LC in the order they were numbered, with all control samples analyzed first, followed by the *Varroa*-exposed samples. Peptides were separated by nanoliquid chromatography (nanoLC) on a Dionex Ultimate 3000 system (Thermo Fisher Scientific) and analyzed on an Orbitrap Fusion Tribrid mass spectrometer (Thermo Fisher Scientific).

2.3 | Proteomic data evaluation

The data were evaluated with MaxQuant version 2.2.0.0 using LFQ algorithms [28, 29] and the Andromeda search engine [30]. The key criteria used in the data analysis were a false discovery rate (FDR) of 0.01 for proteins and peptides, a minimum length of seven amino acids, a fixed modification (methylthio), and variable modifications of N-terminal protein acetylation and methionine oxidation. The data were locally evaluated against selected databases of nonredundant protein sequences that were downloaded from NCBI on February 13, 2023. Sequences related to the honey bee host and the mite ectoparasite were downloaded from the Reference Sequence protein database (RefSeq, [31]) and consisted of 23,251 sequences from *A. mellifera* (txid7460) and 30,221 sequences from *V. destructor* (txid109461). In addition, 6785 viral sequences restricted to *A. mellifera* (excluding bacteriophages) were downloaded from the NCBI database. The local database is available along with the raw data and result files in MassIVE (see the Data Availability section). The data were processed in Perseus version 2.0.7.0 [32]. Results representing standard contaminants, reverse sequences (decoys), and sequences identified only with modified peptides were discarded. The dataset containing proteins with at least five valid LFQ values in at least one experimental group was further analyzed. The dataset was log2 transformed. Missing LFQ values were replaced from the normal distribution (width 0.3; downshift 1.8) and histograms before and after the data imputation were examined. Heatmap with hierarchical clustering was used to check the uniformity of the sample proteomes between the two subgroups. Significant differences were determined by a permutation-based two-sided *t*-test with an error-corrected *p*-value (FDR = 0.05; S0 = 0.1). The number of randomizations in the analysis was 1000. The results were visualized in a volcano plot, and the significant proteins were exported in tabular form. In addition, the significantly differentially expressed proteins (DEPs) were normalized by z-scores across rows, and hierarchical clustering using average Euclidian distance was performed in OriginPro 2024 (OriginLab, Northampton, MA, USA).

To identify functional protein network interactions, we performed an analysis in STRING v11.5 [33, 34]. The STRING network analysis was performed with the identified 77 *A. mellifera* DEPs, for which a list of the curated gene names (including alternative) was found. The analysis was performed at a confidence of 0.3. Only those terms that were significantly enriched with a Benjamini–Hochberg FDR-corrected *p*-value of less than 0.05 were included. Furthermore, the proteins were analyzed individually to correct and complement automated protein annotations. The representative GenBank accession numbers of the significant proteins were provided with a hyperlink to the NCBI protein database, facilitating direct individual examination via the Conserved Domains Database (CCD) [35]. In addition, we performed individual analyses of the DEPs via the Kyoto Encyclopedia of Genes and Genomes (KEGG) [36], InterPro [37], and UniProt. The information retrieved from these databases was added to the proteins in tabular form and provided with hyperlinks, and the key caption was reflected in the visualization of the STRING analysis to the gene symbols. Finally, all the observed proteome changes, together with reference studies, were used to create a schematic of relevant pathways using BioRender (https://biorender.com).

We analyzed the presence of unique peptides retrieved from a MaxQuant peptide table in the samples and checked whether the peptides in the individual samples were identified by MS/MS or only based on mass matching without MS/MS spectra. To increase the reliability of the identified viruses, we performed a qualitative analysis of the viruses via peptide searches based on MaxQuant intensity values with the disabled match-between-runs option [38].

2.4 | Virome analysis of colonies from the mite source site

Virome analysis was performed on randomly selected bees from the brood comb of the colony that was the source of *Varroa* mites and a neighboring colony at the Blatna site. The modified NetoVIR protocol was utilized as described previously [39]. Briefly, two bees per colony were homogenized in 1 mL of 1x phosphate-buffered saline (PBS) in tubes with 2.8-mm ceramic (zirconium oxide) beads (cat. no. P000911-LYSK0-A, Bertin Technologies, Montigny-le-bretonneux, Ile-de-France, France). Homogenization was performed for 1 min at 3000 rpm with a MINILYSIS tissue homogenizer (Bertin Technologies,

Montigny-le-bretonneux, Ile-de-France, France). The samples were treated with benzonase nuclease and micrococcal nuclease (New England Biolabs, Ipswich, MA, USA), and nucleic acids were subsequently isolated with a QIAamp Viral RNA Mini Kit (QIAGEN, Hilden, Germany). Reverse transcription and the first amplification procedure were performed via a modified WTA2 protocol (MERCK, Rahway, NJ, USA). Libraries were prepared via a modified Nextera XT protocol (Illumina, San Diego, CA, USA). The samples were subsequently sequenced at the KU Leuven Nucleomics Core (VIB), Leuven, Belgium, on the HiSeq2000 platform (Illumina, CA, USA) for 2× cycles, during which 150-bp paired-end reads were obtained. The reads were evaluated with FastQC [40] and subsequently trimmed with Trimmomatic [41]. After another evaluation with FastQC, the reads were assembled with SPAdes [42] with the settings –meta- and -k 21, 33, 55, 77. The contigs obtained were blasted with Diamond [43] against a nonredundant protein database (NCBI, downloaded on September 8, 2022). The reads were subsequently mapped to contigs with bwa-mem2 [44], and CoverM [45] was used to identify the reads mapped to individual contigs. The hits and number of reads that had been mapped were uploaded into KronaTools [46].

3 | RESULTS

3.1 | Survival of bees and mites in the manipulative experiment

All 11 control and 11 *Varroa*-exposed bees survived 72 h of exposure to 50 *Varroa* mites. Nineteen dead mites were found at the end of the experiment, while 31 out of 50 mites remained viable throughout the experiment. Ten bees from each group were then subjected to proteomic analysis.

3.2 | Overall proteomic analysis results

LFQ proteomics revealed 26,343 peptides (Table S1) in all the analyzed samples, which were assigned to 2663 proteins (Table S2A). Using the LFQ algorithm, we found six groups of viral proteins (Table S2B; Section 3.3). In addition, we found several proteins identified by *V. destructor* sequence information, of which those identified only by *V. destructor* sequence information were filtered out from further data analysis. For quantitative analysis of honey bee DEPs, we further filtered the data to a threshold of at least five valid LFQ values in an experimental group, resulting in a dataset of 2421 proteins. The histograms before (Figure S1) and after (Figure S2) the imputation of missing data (width 0.3; downshift 1.8) were both symmetric/unimodal. Exploratory analysis of the proteomes using hierarchical clustering on columns (Figure S3) revealed sample homogeneity in the two experimental groups.

3.3 | Identification of viral proteins

Initial analysis using LFQ algorithms revealed that four protein groups matched polyproteins of DWV origin. Importantly, DWV was identified by a total of 16 unique peptides exclusively expressed by *Varroa*-exposed bees. The high number of MS/MS counts (149 for unique peptides) indicates a high level of DWV-B polyprotein in the treated bees. The polyprotein is a large precursor protein that includes the structural proteins VP1, VP2, VP3 and possibly V4 [47] at the N-terminal domain and nonstructural regions (RNA helicase, a chymotrypsin-like 3C protease, and an RNA-dependent RNA polymerase) at the C-terminal domain [48]. Detailed inspection of the identified peptides revealed that all the peptides mapped to the amino acid sequence of the DWV-B polyprotein (665 identical or closely related sequences at NCBI), of which APP91308 was used as a representative sequence. The peptides covered both the structural and nonstructural domains of the protein. In addition, we identified a single unique peptide with a single amino acid substitution D/N at position 871 that matched the VP1 domain of the DWV-A protein (AMK01489) and a unique peptide with a substitution A/T at position 916 (the VP3 domain) corresponding to the polyprotein AUI41303 (Figure 2, Table S3). Because only a single peptide was found for each protein, the interpretation of these findings is inconclusive.

As quantitative LFQ methods may lead to false negatives, we verified the distribution of viral peptides in control and *Varroa*-treated bees via qualitative analysis based on peptide intensities and mapping to the reference sequence. This analysis confirmed the absence of DWV in the control samples, while all *Varroa*-treated bees were DWV positive (Figure 2, Table S3).

In addition to DWV, LFQ-based analysis revealed the presence of Apis flavivirus (AFV) and Apis mellifera filamentous virus (AmFV), which was confirmed by qualitative analysis. Moreover, the latter analysis suggested the presence of two additional viral species, Kashmir bee virus (KBV) and Bee macula-like virus (BMLV) (Figure 2). Polyprotein of AFV origin (YP_009388303) [49] was detected by two unique peptides found only in four *Varroa*-treated bees, while no AFV infection was observed in the controls. In three control bees, we found two unique peptides that matched the protein of AmFV origin with the C-terminal domain of the putative metallopeptidase (AKY03074). The presence of KBV was suggested by the identification of two overlapping unique peptides that matched a domain of the 3C-protease of the nonstructural KBV protein [50]. These peptides were detected in two control bees and six *Varroa*-treated bees (Figure 2). Finally, BMLV infection was suggested only for a single *Varroa*-treated bee (v5). In this sample, three unique peptides matched the BMLV coat protein (UYM19103). Importantly, all these proteins were identified with very low MS/MS count values (3–8; Figure 2), suggesting a low load of the corresponding viruses in comparison to DWV. Collectively, our data indicate significant *Varroa*-dependent DWV infection in *Varroa*-treated bees. Persistent infections with AFV and BMLV might also be associated with *Varroa*, while infections with KBV and AmFV in our

Virus	Protein ID*	MS/MS Count	Number Peptides	Number Uni Pep**
DWV-B	APP91308	149	129	16
DWV-A	AMK01489	14	60	1
DWV	AUI41303	13	2	1
AFV	AKY03074	3	2	2
AmFV	ARO50047	4	2	2
BMLV+	UYM19103	3	3	3
KBV+	AHL83499	8	2	2

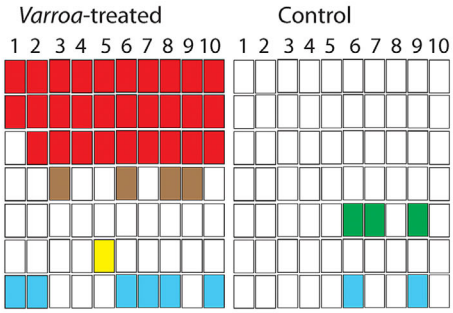

DVW, *Deformed wing virus*
AFV, *Apis flavivirus*
AmFV, *Apis mellifera filamentous virus*
BMLV, *Bee macula-like virus*
KBV, *Kashmir bee virus*

*Accession number of leading peptide in unique protein group
**Uni Pep, number of peptides that belong to unique protein group
+ Identification based on peptide searches

FIGURE 2 Distribution of viruses identified in *Varroa*-treated and control bees by MS/MS identified peptides.

samples seemed to be *Varroa* independent. Importantly, the persistent infections of AFV and BMLV did not compromise the control samples.

3.4 | Virome in *Varroa* source colony and neighboring colony

Identification of viral proteins in *Varroa*-treated samples prompted us to investigate viromes in the *Varroa* source colony and the neighboring colony without any signs of varroosis. Among the viruses that infect honey bees in the *Varroa* source colony, AmFV had the highest abundance (4% of all reads) (Figure S4). The others accounted for less than 1% of the reads. These viruses included Black queen cell virus (BQCV), Varroa/Bee orthomyxovirus-1, and DWV-B. In addition, many other viruses, including bacteriophages and plant-infecting viruses, have been identified, but these are not related to virus transmission by *Varroa*. The virome composition of the neighboring colony (Figure S5) significantly differed. This colony contained overwhelmingly Sacbrood virus (SBV) (23% of all reads) and less than 1% AmFV and BQCV. Although the proportions of DWV-B and Varroa/Bee orthomyxovirus in the virome structure were not high, their presence is important because they are viruses associated with the *Varroa* mite. A comparison of the number of reads for the selected viruses between the collapsing colony (from which the *Varroa* mites were used for the manipulative experiment) and the neighboring colony is shown in Figure 3.

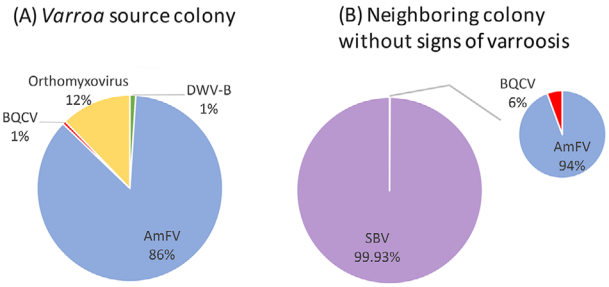

FIGURE 3 Composition of viruses infecting honey bees (%) in (A) the source colony of *Varroa* mites and (B) the colony neighboring the source colony.

3.5 | Effect of *Varroa*/DWV on the bee proteome

Statistical analysis using permutation-based two-sided *t*-test (FDR = 0.05; S0 = 0.1; permutations = 1000) to compare the changes in the proteomes of the 10 *Varroa*-treated and 10 control samples revealed significant changes in 77 bee proteins (Figure 4, Table S4): 50 were downregulated, and 27 were upregulated. This was further reflected in the heatmap of the z-score-transformed data (Figure 5). In the rows, there were two main clusters in which the 27 upregulated proteins and the 50 downregulated proteins clustered together. In the columns, the two subgroups of 10 control and 10 *Varroa*-exposed bees were clustered together, confirming the sample-type uniformity of the identified DEPs.

STRING network analysis of 77 *A. mellifera* DEPs at a confidence level of 0.3 revealed 75 nodes and 59 edges versus 38 expected edges (Figure 6). Note that 75 nodes could be identified among the 77 imputed DEPs because mapping (Table S5) revealed that the protein encoded by the gene *LOC113218812* was not found in STRING; furthermore, our individual verification showed that two proteins (XP_392405.3 and XP_003251576.1) were found under the same gene name (*LOC408875*). The protein-protein interaction (PPI) enrichment *p*-value was 9.87×10^{-4}. Functional enrichment analysis revealed 20 enriched terms (FDR-corrected *p*-value/*q*-value < 0.05) in six categories and all *p*-values corrected for multiple testing within each

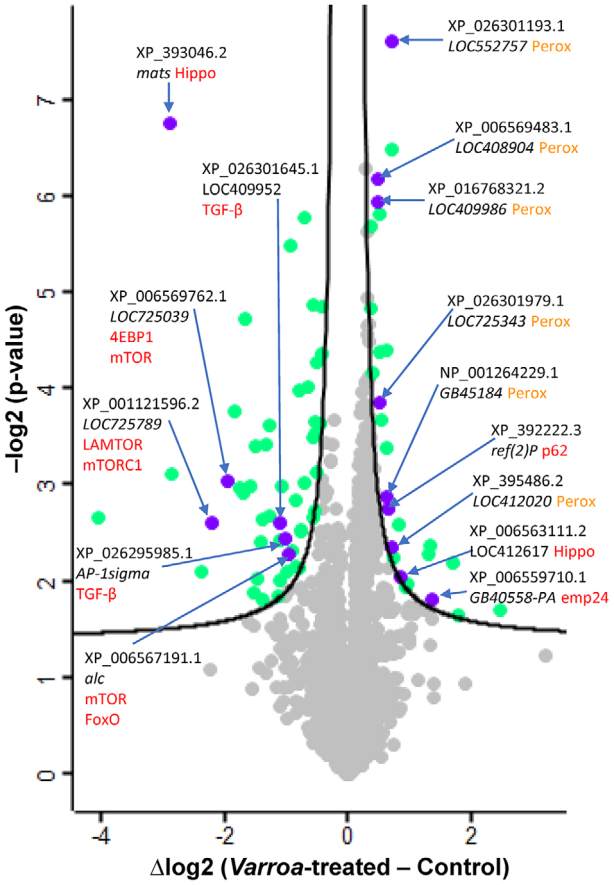

FIGURE 4 Volcano plot identifying 77 significantly (FDR = 0.05; S0 = 0.1; permutations = 1,000) differentially expressed proteins (DEPs) between *Varroa*-treated and control samples of bees. Selected DEPs are labeled in the volcano plot.

category using the Benjamini–Hochberg procedure (FDR) are shown in Table S6.

The most significantly enriched term was the term peroxisomes in the following three categories: cellular component (GO:0005777; 7/91 – observed/background gene count; q-value = 5.2×10^{-4}), KEGG pathways (ame04146; 6/59 – observed/background; q-value = 9.64×10^{-5}), and compartments (GOCC:0005777; 7/93 – observed/background; q-value = 8.9×10^{-4}). In addition, the peroxisome term was combined with other enriched KEGGs: fatty acid metabolism (ame01212; 4/50 – observed/background; q-value = 6.1×10^{-3}), biosynthesis of unsaturated fatty acids (ame01040; 4/27 – observed/background; q-value = 9.9×10^{-4}), β-alanine metabolism (ame00410; 3/21 – observed/background; q-value = 7×10^{-3}), and alpha-linolenic acid metabolism (ame00592; 2/11 – observed/background; q-value = 4.7×10^{-2}). Functional enrichment analysis revealed that structural molecule activity (GO:0005198; 12/355 – observed/background; q-value = 3.6×10^{-4}), was the only significantly enriched term in the category Molecular function. The next important enriched terms were those connected to the cuticle in the Annotated UniProt keywords (KW-0193; 4/42 – observed/background; q-value = 1.05×10^{-2}) and Local STRING network cluster CL19319; 5/92 – observed/background; q-value = 3.71×10^{-2}). Many counts in the network were found in the enriched term "cellular anatomical entity" in two categories: cellular component (GO:0110165; 62/8868 – observed/background; q-value = 1.3×10^{-3}) and compartments (GOCC:0110165; 58/8023 – observed/background; q-value = 4.2×10^{-3}). The results of hyperlinking the individual analysis of the significant proteins in the bioinformatic resources (KEGGs, CDs, InterPro) are shown in Table S7. The key information obtained is reflected in the STRING interaction network (Figure 6) together with the gene symbols.

The key group of interacting proteins in the STRING network (Figure 6) was found to be six peroxisomal proteins. This was supported by the heatmap (Figure 5), which shows the coexpression of the peroxisomal proteins, as five of them clustered immediately next to each other and the sixth clustered nearby. Furthermore, the three nodes directly related to the peroxisomal proteins identified via STRING, that is, proteasomal proteins, proteins involved in steroid degradation and p24, were also upregulated. Notably, p62 was found to be coexpressed in the heatmap, although the direct interaction between p62 and peroxisomal proteins was not detected via STRING. STRING analysis also revealed other groups of interacting DEPs, and the detailed analysis collectively suggested that bee exposure to *Varroa* and consequently DWV infection has an impact on peroxisomal function and cyto-/exoskeleton reorganization and supports the importance of TGF-β signaling and the involvement of the mTORC1 and Hippo pathways in *Varroa*–DWV interactions.

4 | DISCUSSION

4.1 | Original system for investigating the specific developmental stage of bees and *Varroa*/DWV exposure status

In this study, we used a novel, well-defined biological system to investigate the effect of *Varroa*/DWV on the bee proteome. In our system, we used 3-day-old worker bees and particular *Varroa* loads, including the viruses, most notably high levels of DWV in *Varroa*-treated bees. We increased the uniformity of the experimental bees for manipulative experiments by collecting them at the time of emergence [18, 25], ensuring the absence of *Varroa* mites in the cell and on the bees. Thus, since their emergence after the completion of metamorphosis, the experimental bees have had no prior contact with colony members and could not have been contaminated by sharing the feeding route with other bees or the comb, including food stores, as can occur when newly emerged bees are collected collectively from brood combs. In addition, the bees were collected from a single colony with no signs of disease to increase the sample uniformity, but this reduces the biological variability that can be useful in other studies. Importantly, we recorded the number of bees and mites used at the beginning of the experiment and the number that survived. In particular, similar data are required for chronic toxicity tests on bees [51]. Somewhat unexpectedly, all the *Varroa*-exposed bees survived the 72-h treatment, as did

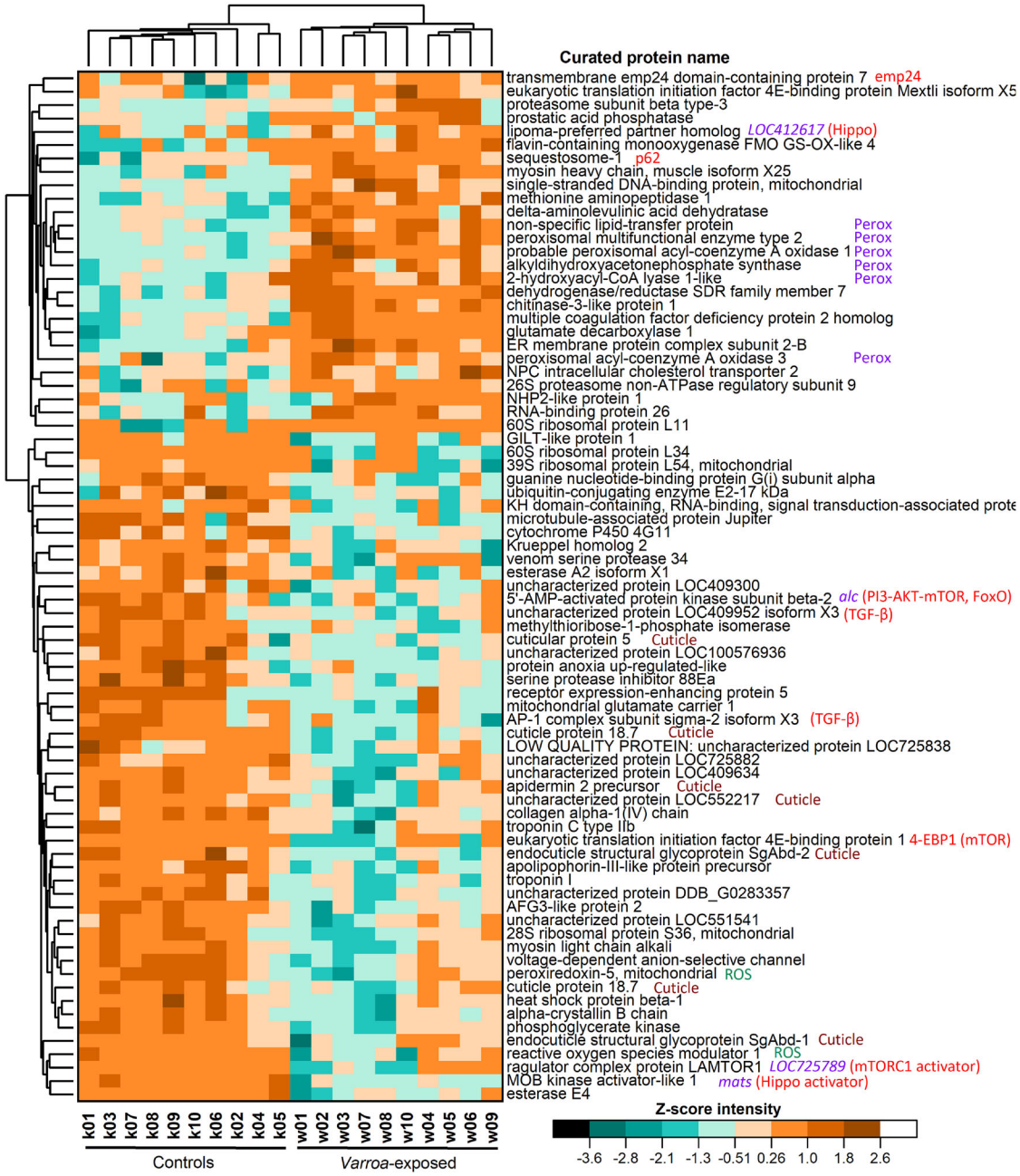

FIGURE 5 Heatmap visualization of the protein expression profiles of all 77 identified DEPs. LFQ values were z-score normalized prior to hierarchical clustering using Euclidean distance in Origin software. In addition to the curated protein names, specific marks are provided for selected proteins.

all the controls. However, there was a 38% loss of live mites during the exposure, which could be due to a decrease in their fitness during the experiment and the previous manipulation, that is, mite collection and placement in the experimental cage. Thus, this study involved *Varroa* parasitization of 11 bees by 31 fully functional mites that were alive at the end of the experiment out of 50 initial mites.

Overall, the results of this study complement those of other studies that have produced similar or different results and interpretations most likely due to differences in study designs and/or analyses of developmental stages, castes, and ages of the bees [23, 24]. For instance, proteomic studies have analyzed the effect of *Varroa* parasitization at the time of emergence [18], in 10-day-old bees [22], in the hemolymph of 1-day-old bees [14], and in worker and drone pupae [52].

4.2 | Virus identification using proteomics

The *Varroa* mite is known to transmit DWV and cause the transition from latent to acute symptomatic DWV infection [2, 53]. In our experiment, we expected a transmitted DWV infection in *Varroa*-exposed

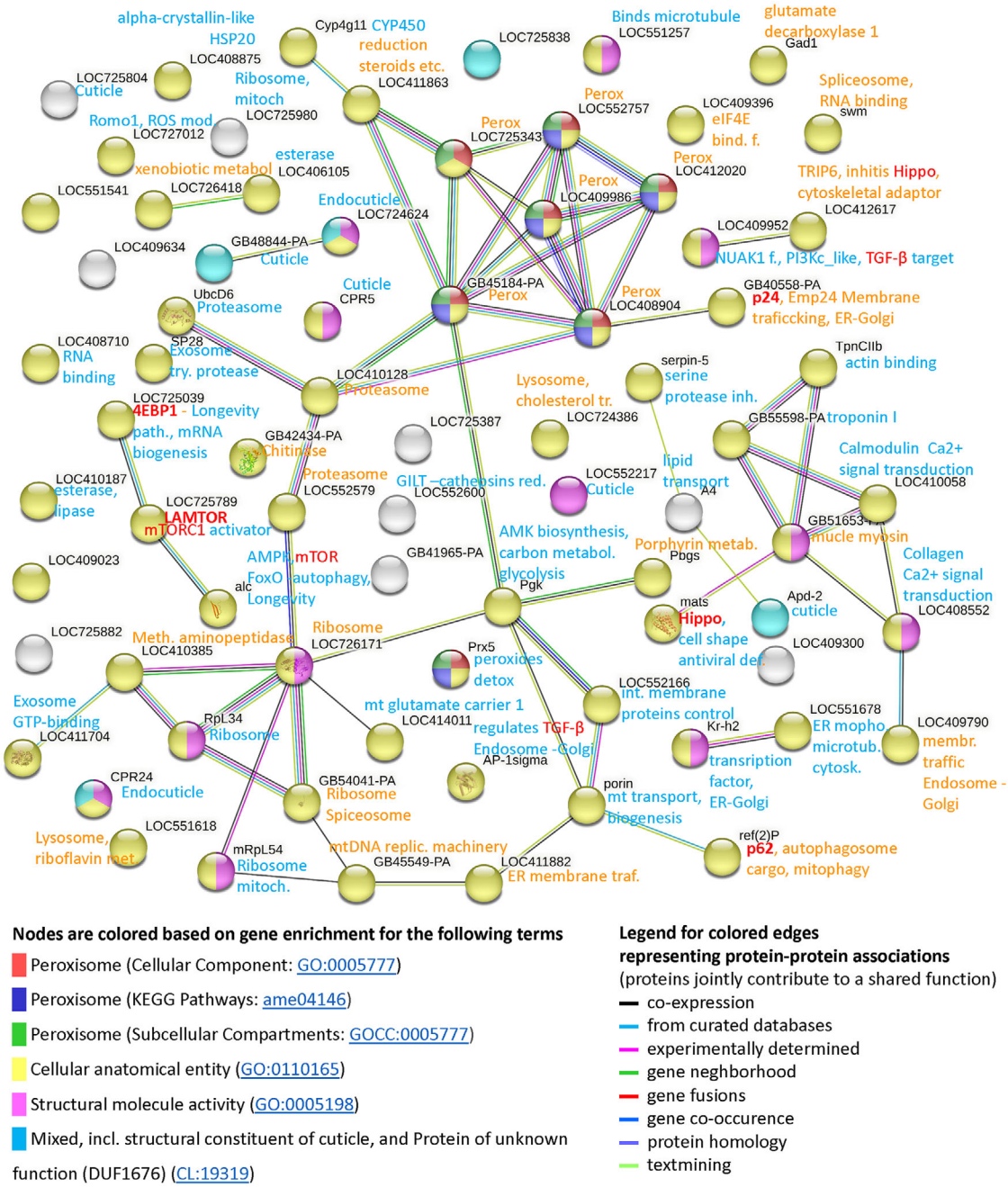

FIGURE 6 Functional protein association network of the significant DEPs determined via STRING. The description added to the gene symbols is derived from the data in Table S7, where annotations from bioinformatic resources (i.e., KEGGs, CDs, InterPro) are provided; orange indicates upregulated DEPs, while blue indicates downregulated DEPs. The red text highlights proteins of specific importance (see Discussion).

bees because the colony from which the mites came showed typical symptoms of varroosis. In addition, we found that the virome of honey bees in the *Varroa*-source colony contained a considerable portion of DWV-B, which is the main genotype associated with *Varroa* occurrence in Europe [54]. Indeed, our proteomic analysis confirmed the presence of DWV-B at high intensity in all 10 *Varroa*-exposed bees, while the virus was not detected in the control bees. For pathogen identification, we exploited the ability of proteomics to identify viral proteins instead of RNA-based qPCR. This approach allowed reliable identification of the viral proteins and host proteins from the same data. Because we endeavored to avoid false-positive identifications of pathogen proteins in honey bees [55], we carefully verified proteins that were identified from the virus alongside honey bee and mite identification. An important issue to address was the occurrence of low LFQ values for the positives for DWV in 6/10 control bees, which could indicate latent DWV infection. However, detailed qualitative analysis revealed that these identifications were based exclusively on the MaxQuant matching-between-runs algorithm, while no MS/MS spectra were recorded for the controls. Thus, DWV in the controls could be considered false positives. In addition, a virus-focused analysis

indicated the presence of persistent viral infection of AmFV, AFV, BMLV, and KBV in some bees. The distribution of viral positives in the bee samples, particularly AmFV and KBV in the controls, suggested that these could be viral legacies that survived metamorphosis in some bees at the time of emergence [15].

4.3 | Pathways affected in bees

The most prominent group of proteins affected by *Varroa*–DWV exposure was a group of peroxisomal proteins, all of which were collectively upregulated. A greater abundance of peroxisomal proteins suggested the upregulation of fatty acid β-oxidation with acyl-CoA oxidase (*LOC412020*; *LOC552757*) and multifunctional enzyme type 2 (*LOC409986*), alpha-oxidation (*GB45184*), the biosynthesis of ether phospholipids (alkyldihydroxyacetonephosphate synthase; *LOC725343*), and lipid transfer (sterol carrier protein-2; *LOC408904*). In general, peroxisomes play key roles in diverse cellular processes, including fatty acid/lipid and amino acid metabolism and the maintenance of reactive oxygen species (ROS) [56–58]. Peroxisomes are functionally and in some cases physically associated with other organelles, including the endoplasmic reticulum (ER), lysosomes, autophagosomes, mitochondria, and lipid droplets [57, 59, 60]. However, peroxisomes are less known for functioning as cell signaling organelles, and ROS generated by peroxisomes can activate intracellular signaling cascades [58, 61]. The observed DEPs suggested that these peroxisome-related functions, whether affected by peroxisomes or those affecting peroxisomes, were modulated by pathogen exposure, as depicted in Figure 7.

Increased peroxisomal metabolism is associated with increased production of ROS that should be eliminated; however, the downregulation of peroxiredoxin-5 (*Prx5*) observed by us and others [62] suggests the opposite. This downregulation may be part of the response to inflammation [62]; in particular, a trade-off has been observed between the protective role of Prx5 in immune and antioxidant functions [63]. Furthermore, one of the critical regulators of ROS is mitochondrial reactive oxygen species modulator 1 (Romo1; *LOC727012*), whose downregulation suggests an attempt to decrease cellular ROS levels [64] and reduce NF-κB activation caused by DWV, as viral infections can increase oxidative stress through Romo1 associated with NF-κB [65]. Taken together, these results suggest that the downregulation of both Prx5 and Romo1 is associated with the immune response to DWV through the modulation of ROS levels, which act as active signaling molecules.

Upregulated transmembrane emp24 domain-containing protein 7 (Tmed7; *GB40558-PA*) is associated with Toll-like receptor 4 (TLR4)-mediated viral infection [66], as it is required for TLR4 trafficking from the ER through the Golgi to the cell surface [67]. Notably, emp24/p24 localizes to the ER, Golgi, COP vesicles, and peroxisomes [68]. Upregulated sequestosome-1 (p62/SQSMT1; *ref(2)P*) is an autophagy receptor that connects autophagosomes to peroxisomes via ubiquitinated peroxisomal PEX5 [59]. Furthermore, p62 was found to be required for the autophagic clearance of ubiquitinated proteins and for the delivery of ubiquitinated cargo to the proteasome, and its levels correlated with autophagic degradation [69]. Incidentally, according to our STRING analysis, proteasomal proteins (*LOC410128*; *LOC552579*) that are connected to peroxisomal proteins were upregulated.

In *Varroa*-exposed bees, we found substantial downregulation of the Ragulator complex protein LAMTOR1 (Lamtor1/p18; *LOC725789*), which is involved in amino acid sensing and activation of mTORC1 [70, 71]. This finding suggested an increase in autophagy, particularly pexophagy [58, 72]. In addition, suppression of mTORC1 activity has been linked to alterations in cholesterol transport [73], the hijacking (i.e., upregulation of NPC2; *LOC724386*) of which is essential for infection and the life cycle [74]. Because of the link to the nutrient-sensing pathway, the collective changes in the mTORC1 pathway and peroxisomal β-oxidation [75] may explain the increase in the sphingolipid metabolic rate observed by Kunc et al. [22] in 10 day old parasitized bees.

A downregulated Lamtor1/p18 was a key marker in our study. According to the STRING analysis, it interacts with eukaryotic translation initiation factor 4E-binding protein 1 (4E-BP1; *LOC725039*), which was downregulated to a similar extent. Importantly, 4E-BP1 harbors numerous phosphorylation sites, and this phosphorylation is regulated by the mTOR pathway [76], suggesting that this effect is important for our interpretation (Figure 7). mTORC1 stimulates translation via phosphorylation of 4E-BP1 [77, 78]. 4E-BP1 binds eIF4E, through which some viruses modulate protein synthesis; in particular, picornaviruses (which include DWV) induce the dephosphorylation of 4E-BP, leading to cap-dependent inhibition of protein synthesis [79]. According to our data, 4E-BP1 was downregulated and may have been affected by dephosphorylation triggered by viral activity [80–82]. Importantly, the mTORC1/4E-BP1 axis is related to TGF-β-induced pathways and has been identified as a key pathway involved in wound healing and repair [83, 84]. Injury-induced mTOR activation in epithelial cells is likely conserved across species, that is, insects and vertebrates [85]. Furthermore, Lamtor1/p18 was linked in STRING to a regulatory subunit (PRKAB2; *alc*) of AMP-activated protein kinase (AMPK), which directly regulates cell growth and macroautophagy and microautophagy via mTORC1. This function has also been linked to the aforementioned p62 [86].

We found that some DEPs were directly related to TGF-β, a signaling pathway that regulates cell proliferation, differentiation, and apoptosis and is important for inflammation, various immune responses against microbes, and wound healing [87–90]. TGF-β has been suggested to play an important role in *Varroa*-parasitized bees at the time of emergence [18]. It has been shown that there is crosstalk between the TGF-β, Hippo, and mTORC1 pathways [91–93]. Thus, the downregulation of MOB kinase activator-like 1 (MOB1; *mats*), a key signaling adaptor of the Hippo pathway, which is essential for organ growth control and tissue homeostasis, is important in this context [94]. Since MOB1 was previously shown to be upregulated in *Varroa*–DWV variant emerging bees [18], we suggest that differentially regulated MOB1 may be associated with differentially altered innate immune defenses [95, 96] in two different developmental stages (3-day-old bees vs. emerging bees). Notably, modulation of the Hippo pathway interferes

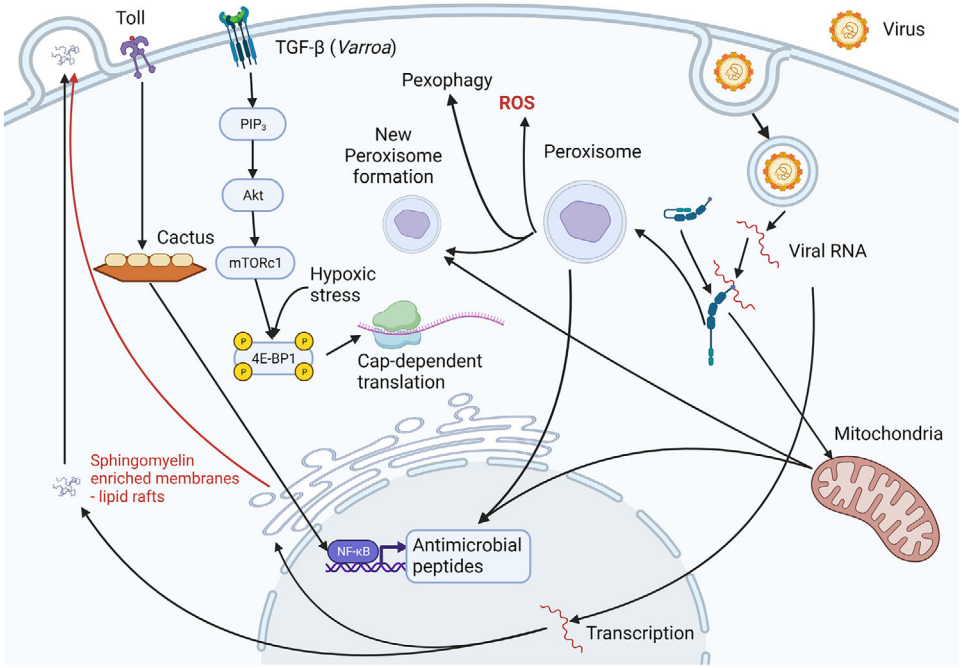

FIGURE 7 The overall scheme of host pathways affected by *Varroa*/DWV exposure. The scheme summarizes the results of this study and accounts for the previous studies that have been conducted. The effect of picornavirus multiplication on both peroxisomes and mitochondria is suggested, as is the cell antiviral response via the Toll signaling pathway. Furthermore, peroxisome signaling is associated with ROS production and pexophagy. In addition, the results indicated that the TGF-β pathway is affected by *Varroa* feeding on the host and plays a role in DWV infection. An important factor that is likely to affect viral replication is impaired autophagy, which is associated with stress (mainly due to *Varroa* parasitization) that affects mTORC1.

with antiviral defenses [97, 98], which are likely differentially regulated in the two different developmental stages.

The impact of *Varroa* and/or DWV on cyto-/exoskeleton reorganization has been previously identified, and the relevant markers in our study included changes in cuticle and cytoskeletal proteins, including muscle proteins [14, 18, 52, 99]. In this context, through direct interaction via STRING, we found MOB1 in the Hippo pathway [100]. Furthermore, the Lipoma-preferred partner TRIP6 [101]; *LOC412617*), which is involved in the Hippo pathway, affects actin cytoskeletal reorganization, cell adhesion and migration [102]. The function of TRIP6 is linked to another protein (NUAK1; *LOC409952*) that is a TGF-β target. The downregulation of the microtubule-associated protein Jupiter (*LOC551257*) plays an important role in microtubule stability in *Drosophila* [103, 104]. Overall, changes related to cytoskeletal remodeling may be linked primarily to the DWV life cycle since viruses need to hijack cytoplasmic membrane trafficking machines for their own replication, assembly and release from a cell [105–109]. However, cytoskeleton remodeling is also due to *Varroa* syndrome affecting some of these pathways, and the interplay among these pathways leads to synergistic effects with DWV during parasite sucking of a host [18].

The number of downregulated proteins was related to the structural constituents of the cuticle (*LOC724624*, *CPR24*, *CPR5*, *GB48844*, *LOC725804*, *LOC552217*, *Apd-2*, and *Cyp4g11*). Like in our study, *Varroa*-parasitized purple-eye pupae exhibited a downregulated array of cuticular proteins [52]. Additionally, parasitization of honey bees by *Vairimorpha* (*Nosema*) *ceranae* (5 days postinfection) downregulated seven cuticle genes [110], some of which were the same as those in our study. Changes in exoskeletal proteins due to infection with DWV might be linked to weakening of the external barrier of a host to facilitate transmission [110]; however, transmission of this virus has been connected mainly to the ectoparasite *Varroa*, which creates wounds [111] and delays healing in a host [18]. Interestingly, differences in the expression of cuticle genes have been implicated in different hygienic behaviors of honey bees [112] and resistance to DWV infection [99].

An important change affecting immunity is the downregulation of the serine protease inhibitor 88Ea (serpin-5; *serpin-5*), which has been shown to regulate prophenoloxidase (PPO) activation and antimicrobial peptide pathway activation. Serpin-5 has been shown to function as a secreted negative modulator of Toll signaling [113, 114]. It also acts as a component of the extracellular surveillance system in epithelial cells, and the mechanism has been linked to the Hippo pathway [115].

Overall, our observations summarized in Figure 7 are in agreement with the following previous results on the effect of *Varroa*–DWV on bees: (1) the levels of lipid metabolism-related proteins increase in parasitized worker pupae [52]; (2) the levels of proteins related to the metabolism of lipids and branched amino acids increase in the hemolymph of *Varroa*-parasitized bees [14]; and (3) the sphingolipid metabolism rate increases in *Varroa*-parasitized 10-day-old bees [22]. Some of the contrasting differences in expression levels nicely illustrate the influence of the experimental design. For instance, the opposite regulatory effects on Lamtor1/p18 and MOB1 illustrate the influence of the experimental design and the age of the bees analyzed

on the results; that is, 3-day-old with 3 days of *Varroa*–DWV exposure (this study) vs. 0-day-old (emerging) [18].

5 | CONCLUSION

This study investigated the effect of *Varroa*–DWV exposure on honey bees in a specific manipulative experiment. High-throughput proteomics revealed certain characteristics that allowed the identification of markers and pathways affected by *Varroa*–DWV interaction in 3-day-old bees postemergence. We found that a key set of affected proteins was associated with increased peroxisomal metabolism, and the other proteomic changes, such as ROS homeostasis/signaling, were also associated with peroxisomes. These results are consistent with the finding that peroxisomes play an important role in viral infections. In the future, it will be necessary to determine to what extent peroxisomes act as antiviral agents or whether they also exert proviral functions in honey bees parasitized by *Varroa*. These results also support the importance of TGF-β signaling in the *Varroa*–DWV interaction and reveal the link between the mTORC1 and Hippo pathways. The ability of *Varroa* to promote DWV infection likely occurs through the subversion of host autophagy caused by the modulation of apoptosis and proliferation associated with the suppression of wound healing and repair by *Varroa* and the reprogramming of cellular functions by DWV. Cytoskeletal remodeling and changes in cuticular proteins seem to be concomitant processes associated with viral infection and *Varroa* feeding on the host. The limitation of this study is that whole bees were analyzed, and in the future, it will be necessary to localize the changes to specific cell types and tissues.

AUTHOR CONTRIBUTIONS

Tomas Erban wrote the main manuscript, designed the study, and evaluated the data in detail. Klara Kadlikova processed the samples. Karel Harant and Pavel Talacko performed the nano-LC–MS/MS analysis. Jan Tachezy and Karel Harant contributed to the data evaluation. Dominika Kadleckova, Martina Salakova, and Ruth Tachezy performed and evaluated the virome analysis. Bruno Sopko created the scheme of affected pathways. Martin Markovic verified the references, edited the draft version and checked the formality. Jan Tachezy, Ruth Tachezy, Dominika Kadleckova, and Martina Salakova contributed to the writing. All the authors have read and approved the manuscript.

ACKNOWLEDGMENTS

The authors are grateful to the beekeepers for allowing us to collect the mite and bee samples. This research was supported by project no. QK1910018 (NAZV), Institutional Support for R&D no. MZE-RO0423 of the Ministry of Agriculture of the Czech Republic, the Charles University grant number SVV 260679 and ERDF project CePaViP no. CZ.02.1.01/0.0/0.0/16_019/0000759.

CONFLICT OF INTEREST STATEMENT

The authors declare that they have no known competing financial interests or personal relationships that could have appeared to influence the work reported in this paper.

DATA AVAILABILITY STATEMENT

The raw data from the nanoLC–MS/MS runs, peak list files, search database, search engine parameters and zipped combined_txt from MaxQuant can be accessed via the complete MassIVE MSV000094006 submission (doi:10.25345/C5H12VJ8N) or ProteomeXchange (PXD049168). The reads from the virome analysis were deposited into the NCBI database (PRJNA943204, SRR23800994-5).

ORCID

Tomas Erban https://orcid.org/0000-0003-1730-779X
Dominika Kadleckova https://orcid.org/0000-0002-4312-7373
Bruno Sopko https://orcid.org/0000-0002-5580-1871
Karel Harant https://orcid.org/0000-0002-9654-5392
Pavel Talacko https://orcid.org/0000-0002-0943-4564
Martin Markovic https://orcid.org/0000-0003-3435-1215
Martina Salakova https://orcid.org/0000-0003-0827-1211
Klara Kadlikova https://orcid.org/0000-0002-9321-9380
Ruth Tachezy https://orcid.org/0000-0001-7689-9727
Jan Tachezy https://orcid.org/0000-0001-6976-8446

REFERENCES

1. Anderson, D. L., & Trueman, J. W. H. (2000). *Varroa jacobsoni* (Acari: Varroidae) is more than one species. *Experimental and Applied Acarology*, *24*(3), 165–189. https://doi.org/10.1023/A:1006456720416
2. Traynor, K. S., Mondet, F., de Miranda, J. R., Techer, M., Kowallik, V., Oddie, M. A. Y., Chantawannakul, P., & Mcafee, A. (2020). *Varroa destructor*: A complex parasite, crippling honey bees worldwide. *Trends in Parasitology*, *36*(7), 592–606. https://doi.org/10.1016/j.pt.2020.04.004
3. Australian Government (2022). *Varroa* mite (*Varroa destructor*): pest situation. National pest & disease outbreaks. (Accessed date: 9 March 2023). https://www.outbreak.gov.au/current-responses-to-outbreaks/varroa-mite
4. Rooth, M. (2018). *Varroa* mite detected at Port of Melbourne on a ship from United States. *ABC Rural*, 29 June 2018. https://www.abc.net.au/news/rural/2018-06-29/varroa-mite-detected-in-melbourne/9923972
5. Martin, S. J. (2001). The role of *Varroa* and viral pathogens in the collapse of honeybee colonies: a modelling approach. *Journal of Applied Ecology*, *38*(5), 1082–1093. https://doi.org/10.1046/j.1365-2664.2001.00662.x
6. Rosenkranz, P., Aumeier, P., & Ziegelmann, B. (2010). Biology and control of *Varroa destructor*. *Journal of Invertebrate Pathology*, *103*(Supplement 1), S96–S119. https://doi.org/10.1016/j.jip.2009.07.016
7. Wilfert, L., Long, G., Leggett, H. C., Schmid-Hempel, P., Butlin, R., Martin, S. J. M., & Boots, M. (2016). Deformed wing virus is a recent global epidemic in honeybees driven by *Varroa* mites. *Science*, *351*(6273), 594–597. https://doi.org/10.1126/science.aac9976
8. Roberts, J. M. K., Anderson, D. L., & Durr, P. A. (2018). Metagenomic analysis of *Varroa*-free Australian honey bees (*Apis mellifera*) shows a diverse Picornavirales virome. *Journal of General Virology*, *99*(6), 818–826. https://doi.org/10.1099/jgv.0.001073
9. Kadleckova, D., Tachezy, R., Erban, T. S., Deboutte, W., Nunvar, J., Salakova, M., & Matthijnssens, J. (2022). The virome of healthy honey bee colonies: ubiquitous occurrence of known and new viruses in bee populations. *mSystems*, *7*(3), e0007222. https://doi.org/10.1128/msystems.00072-22
10. Bowen-Walker, P. L., & Gunn, A. (2001). The effect of the ectoparasitic mite, *Varroa destructor* on adult worker honeybee (*Apis mellifera*) emergence weights, water, protein, carbohydrate, and lipid levels.

Entomologia Experimentalis et Applicata, *101*(3), 207–217. https://doi.org/10.1046/j.1570-7458.2001.00905.x

11. Erban, T., Harant, K., Hubalek, M., Vitamvas, P., Kamler, M., Poltronieri, P., Tyl, J., Markovic, M., & Titera, D. (2015). In-depth proteomic analysis of *Varroa destructor*: Detection of DWV-complex, ABPV, VdMLV and honeybee proteins in the mite. *Scientific Reports*, *5*(1), 13907. https://doi.org/10.1038/srep13907
12. McAfee, A., Chan, Q. W. T., Evans, J., & Foster, L. J. (2017). A *Varroa destructor* protein atlas reveals molecular underpinnings of developmental transitions and sexual differentiation. *Molecular & Cellular Proteomics*, *16*(12), 2125–2137. https://doi.org/10.1074/mcp.RA117.000104
13. Ramsey, S. D., Ochoa, R., Bauchan, G., Gulbronson, C., Mowery, J. D., Cohen, A., Lim, D., Joklik, J., Cicero, J. M., Ellis, J. D., Hawthorne, D., & Vanengelsdorp, D. (2019). *Varroa destructor* feeds primarily on honey bee fat body tissue and not hemolymph. *Proceedings of the National Academy of Sciences of the United States of America*, *116*(5), 1792–1801. https://doi.org/10.1073/pnas.1818371116
14. Slowinska, M., Nynca, J., Bak, B., Wilde, J., Siuda, M., & Ciereszko, A. (2019). 2D-DIGE proteomic analysis reveals changes in haemolymph proteome of 1-day-old honey bee (*Apis mellifera*) workers in response to infection with *Varroa destructor* mites. *Apidologie*, *50*(5), 632–656. https://doi.org/10.1007/s13592-019-00674-z
15. Yang, X., & Cox-Foster, D. L. (2005). Impact of an ectoparasite on the immunity and pathology of an invertebrate: Evidence for host immunosuppression and viral amplification. *Proceedings of the National Academy of Sciences of the United States of America*, *102*(21), 7470–7475. https://doi.org/10.1073/pnas.0501860102
16. Di Prisco, G., Annoscia, D., Margiotta, M., Ferrara, R., Varricchio, P., Zanni, V., Caprio, E., Nazzi, F., & Pennacchio, F. (2016). A mutualistic symbiosis between a parasitic mite and a pathogenic virus undermines honey bee immunity and health. *Proceedings of the National Academy of Sciences of the United States of America*, *113*(12), 3203–3208. https://doi.org/10.1073/pnas.1523515113
17. Nazzi, F., Brown, S. P., Annoscia, D., Del Piccolo, F., Di Prisco, G., Varricchio, P., Della Vedova, G., Cattonaro, F., Caprio, E., & Pennacchio, F. (2012). Synergistic parasite-pathogen interactions mediated by host immunity can drive the collapse of honeybee colonies. *PLOS Pathogens*, *8*(6), e1002735. https://doi.org/10.1371/journal.ppat.1002735
18. Erban, T., Sopko, B., Kadlikova, K., Talacko, P., & Harant, K. (2019). *Varroa destructor* parasitism has a greater effect on proteome changes than the deformed wing virus and activates TGF-β signaling pathways. *Scientific Reports*, *9*(1), 9400. https://doi.org/10.1038/s41598-019-45764-1
19. Kuster, R. D., Boncristiani, H. F., & Rueppell, O. (2014). Immunogene and viral transcript dynamics during parasitic *Varroa destructor* mite infection of developing honey bee (*Apis mellifera*) pupae. *Journal of Experimental Biology*, *217*(10), 1710–1718. https://doi.org/10.1242/jeb.097766
20. Navajas, M., Migeon, A., Alaux, C., Martin-Magniette, M. L., Robinson, G. E., Evans, J. D., Cros-Arteil, S., Crauser, D., & Le Conte, Y. (2008). Differential gene expression of the honey bee *Apis mellifera* associated with *Varroa destructor* infection. *BMC Genomics*, *9*(1), 301. https://doi.org/10.1186/1471-2164-9-301
21. Johnson, R. M., Evans, J. D., Robinson, G. E., & Berenbaum, M. R. (2009). Changes in transcript abundance relating to colony collapse disorder in honey bees (*Apis mellifera*). *Proceedings of the National Academy of Sciences of the United States of America*, *106*(35), 14790–14795. https://doi.org/10.1073/pnas.0906970106
22. Kunc, M., Dobes, P., Ward, R., Lee, S., Cegan, R., Dostalkova, S., Holusova, K., Hurychova, J., Elias, S., Pindakova, E., Cukanova, E., Prodelalova, J., Petrivalsky, M., Danihlik, J., Havlik, J., Hobza, R., Kavanagh, K., & Hyrsl, P. (2023). Omics-based analysis of honey bee (*Apis mellifera*) response to *Varroa* sp. parasitisation and associated factors reveals changes impairing winter bee generation. *Insect Biochemistry and Molecular Biology*, *152*, 103877. https://doi.org/10.1016/j.ibmb.2022.103877
23. Ryabov, E. V., Wood, G. R., Fannon, J. M., Moore, J. D., Bull, J. C., Chandler, D., Mead, A., Burroughs, N., & Evans, D. J. (2014). A virulent strain of deformed wing virus (DWV) of honeybees (*Apis mellifera*) prevails after *Varroa destructor*-mediated, or *in vitro*, transmission. *PLOS Pathogens*, *10*(6), e1004230. https://doi.org/10.1371/journal.ppat.1004230
24. Doublet, V., Poeschl, Y., Gogol-Doring, A., Alaux, C., Annoscia, D., Aurori, C., Barribeau, S. M., Bedoya-Reina, O. C., Brown, M. J. F., Bull, J. C., Flenniken, M. L., Galbraith, D. A., Genersch, E., Gisder, S., Grosse, I., Holt, H. L., Hultmark, D., Lattorff, H. M. G., Le Conte, Y., … Grozinger, C. M. (2017). Unity in defence: Honeybee workers exhibit conserved molecular responses to diverse pathogens. *BMC Genomics*, *18*(1), 207. https://doi.org/10.1186/s12864-017-3597-6
25. Erban, T., Harant, K., Kamler, M., Markovic, M., & Titera, D. (2016). Detailed proteome mapping of newly emerged honeybee worker hemolymph and comparison with the red-eye pupal stage. *Apidologie*, *47*(6), 805–817. https://doi.org/10.1007/s13592-016-0437-7
26. Erban, T., Parizkova, K., Sopko, B., Talacko, P., Markovic, M., Jarosova, J., & Votypka, J. (2023). Imidacloprid increases the prevalence of the intestinal parasite *Lotmaria passim* in honey bee workers. *Science of The Total Environment*, *905*, 166973. https://doi.org/10.1016/j.scitotenv.2023.166973
27. Erban, T., Sopko, B., Talacko, P., Harant, K., Kadlikova, K., Halesova, T., Riddellova, K., & Pekas, A. (2019). Chronic exposure of bumblebees to neonicotinoid imidacloprid suppresses the entire mevalonate pathway and fatty acid synthesis. *Journal of Proteomics*, *196*, 69–80. https://doi.org/10.1016/j.jprot.2018.12.022
28. Cox, J., & Mann, M. (2008). MaxQuant enables high peptide identification rates, individualized p.p.b.-range mass accuracies and proteome-wide protein quantification. *Nature Biotechnology*, *26*(12), 1367–1372. https://doi.org/10.1038/nbt.1511
29. Cox, J., Hein, M. Y., Luber, C. A., Paron, I., Nagaraj, N., & Mann, M. (2014). Accurate proteome-wide label-free quantification by delayed normalization and maximal peptide ratio extraction, termed MaxLFQ. *Molecular & Cellular Proteomics*, *13*(9), 2513–2526. https://doi.org/10.1074/mcp.M113.031591
30. Cox, J., Neuhauser, N., Michalski, A., Scheltema, R. A., Olsen, J. V., & Mann, M. (2011). Andromeda: A peptide search engine integrated into the MaxQuant environment. *Journal of Proteome Research*, *10*(4), 1794–1805. https://doi.org/10.1021/pr101065j
31. O'Leary, N. A., Wright, M. W., Brister, J. R., Ciufo, S., Haddad, D., Mcveigh, R., Rajput, B., Robbertse, B., Smith-White, B., Ako-Adjei, D., Astashyn, A., Badretdin, A., Bao, Y., Blinkova, O., Brover, V., Chetvernin, V., Choi, J., Cox, E., Ermolaeva, O., … Pruitt, K. D. (2016). Reference sequence (RefSeq) database at NCBI: current status, taxonomic expansion, and functional annotation. *Nucleic Acids Research*, *44*(D1), D733–D745. https://doi.org/10.1093/nar/gkv1189
32. Tyanova, S., Temu, T., Sinitcyn, P., Carlson, A., Hein, M. Y., Geiger, T., Mann, M., & Cox, J. (2016). The Perseus computational platform for comprehensive analysis of (prote)omics data. *Nature Methods*, *13*(9), 731–740. https://doi.org/10.1038/nmeth.3901
33. Szklarczyk, D., Gable, A. L., Lyon, D., Junge, A., Wyder, S., Huerta-Cepas, J., Simonovic, M., Doncheva, N. T., Morris, J. H., Bork, P., Jensen, L. J., & von Mering, C. (2019). STRING v11: protein–protein association networks with increased coverage, supporting functional discovery in genome-wide experimental datasets. *Nucleic Acids Research*, *47*(D1), D607–D613. https://doi.org/10.1093/nar/gky1131
34. Szklarczyk, D., Kirsch, R., Koutrouli, M., Nastou, K., Mehryary, F., Hachilif, R., Gable, A. L., Fang, T., Doncheva, N. T., Pyysalo, S., Bork, P., Jensen, L. J., & von Mering, C. (2023). The STRING database in 2023: protein–protein association networks and functional enrichment analyses for any sequenced genome of interest.

Nucleic Acids Research, *51*(D1), D638–D646. https://doi.org/10.1093/nar/gkac1000

35. Lu, S., Wang, J., Chitsaz, F., Derbyshire, M. K., Geer, R. C., Gonzales, N. R., Gwadz, M., Hurwitz, D. I., Marchler, G. H., Song, J. S., Thanki, N., Yamashita, R. A., Yang, M., Zhang, D., Zheng, C., Lanczycki, C. J., & Marchler-Bauer, A. (2020). CDD/SPARCLE: The conserved domain database in 2020. *Nucleic Acids Research*, *48*(D1), D265–D268. https://doi.org/10.1093/nar/gkz991
36. Kanehisa, M., Furumichi, M., Sato, Y., Kawashima, M., & Ishiguro-Watanabe, M. (2023). KEGG for taxonomy-based analysis of pathways and genomes. *Nucleic Acids Research*, *51*(D1), D587–D592. https://doi.org/10.1093/nar/gkac963
37. Paysan-Lafosse, T., Blum, M., Chuguransky, S., Grego, T., Pinto, B. L., Salazar, G. A., Bileschi, M. L., Bork, P., Bridge, A., Colwell, L., Gough, J., Haft, D. H., Letunic, I., Marchler-Bauer, A., Mi, H., Natale, D. A., Orengo, C. A., Pandurangan, A. P., Rivoire, C., … Bateman, A. (2023). InterPro in 2022. *Nucleic Acids Research*, *51*(D1), D418–D427. https://doi.org/10.1093/nar/gkac993
38. Lim, M. Y., Paulo, J. A., & Gygi, S. P. (2019). Evaluating false transfer rates from the match-between-runs algorithm with a two-proteome model. *Journal of Proteome Research*, *18*(11), 4020–4026. https://doi.org/10.1021/acs.jproteome.9b00492
39. Conceicao-Neto, N., Yinda, K. C., Van Ranst, M., & Matthijnssens, J. (2018). *NetoVIR: modular approach to customize sample preparation procedures for viral metagenomics*. In: A. Moya, & V. P. Brocal (Eds.), The human virome (pp. 85–95). New York, NY: Humana Press. https://doi.org/10.1007/978-1-4939-8682-8_7
40. Babraham Bioinformatics. (2019). FastQC. Cambridge: Babraham Institute. (Accessed date: 9 March 2023). https://www.bioinformatics.babraham.ac.uk/projects/fastqc/
41. Bolger, A. M., Lohse, M., & Usadel, B. (2014). Trimmomatic: A flexible trimmer for Illumina sequence data. *Bioinformatics*, *30*(15), 2114–2120. https://doi.org/10.1093/bioinformatics/btu170
42. Bankevich, A., Nurk, S., Antipov, D., Gurevich, A. A., Dvorkin, M., Kulikov, A. S., Lesin, V. M., Nikolenko, S. I., Pham, S., Prjibelski, A. D., Pyshkin, A. V., Sirotkin, A. V., Vyahhi, N., Tesler, G., Alekseyev, M. A., & Pevzner, P. A. (2012). SPAdes: A new genome assembly algorithm and its applications to single-cell sequencing. *Journal of Computational Biology*, *19*(5), 455–477. https://doi.org/10.1089/cmb.2012.0021
43. Buchfink, B., Reuter, K., & Drost, H. G. (2021). Sensitive protein alignments at tree-of-life scale using DIAMOND. *Nature Methods*, *18*(4), 366–368. https://doi.org/10.1038/s41592-021-01101-x
44. Vasimuddin, M., Misra, S., Li, H., & Aluru, S. (2019). Efficient architecture-aware acceleration of BWA-MEM for multicore systems. In: L. Alvarez, L. Arantes, E. Arima, T. Benson, J. L. Bez, S. Bhalachandra, … A. Zlateski (Eds.), 2019 IEEE 33rd International Parallel and Distributed Processing Symposium (IPDPS 2019) (pp. 314–324). https://doi.org/10.1109/ipdps.2019.00041
45. Woodcroft, B. J. (2021). CoverM. GitHub. (Accessed date: 9 March 2023). https://github.com/wwood/CoverM
46. Ondov, B. D., Bergman, N. H., & Phillippy, A. M. (2011). Interactive metagenomic visualization in a web browser. *BMC Bioinformatics*, *12*(1), 385. https://doi.org/10.1186/1471-2105-12-385
47. Skubnik, K., Novacek, J., Fuzik, T., Pridal, A., Paxton, R. J., & Plevka, P. (2017). Structure of deformed wing virus, a major honey bee pathogen. *Proceedings of the National Academy of Sciences of the United States of America*, *114*(12), 3210–3215. https://doi.org/10.1073/pnas.1615695114
48. Lanzi, G., de Miranda, J. R., Boniotti, M. B., Cameron, C. E., Lavazza, A., Capucci, L., Camazine, S. M., & Rossi, C. (2006). Molecular and biological characterization of deformed wing virus of honeybees (*Apis mellifera* L.). *Journal of Virology*, *80*(10), 4998–5009. https://doi.org/10.1128/JVI.80.10.4998-5009.2006
49. Remnant, E. J., Shi, M., Buchmann, G., Blacquiere, T., Holmes, E. C., Beekman, M., & Ashe, A. (2017). A diverse range of novel RNA viruses in geographically distinct honey bee populations. *Journal of Virology*, *91*(16), e00158–00117. https://doi.org/10.1128/jvi.00158-17
50. Reddy, K. E., Yoo, M.-S., Kim, Y.-H., Kim, N.-H., Jung, H.-N., Thao, L. T. B., Ramya, M., Doan, H. T. T., Nguyen, L. T. K., Jung, S.-C., & Kang, S.-W. (2014). Analysis of the RdRp, intergenic and structural polyprotein regions, and the complete genome sequence of Kashmir bee virus from infected honeybees (*Apis mellifera*) in Korea. *Virus Genes*, *49*(1), 137–144. https://doi.org/10.1007/s11262-014-1074-8
51. Organisation for Economic Co-operation and Development (OECD). (2017). Test No. *245*: Honey bee (Apis mellifera L.), chronic oral toxicity test (10-day feeding). In: OECD (Ed.), OECD guidelines for the testing of chemicals, section 2: Effects on biotic systems. Paris: OECD Publishing. https://www.oecd-ilibrary.org/environment/test-no-245-honey-bee-apis-mellifera-l-chronic-oral-toxicity-test-10-day-feeding_9789264284081-en
52. Surlis, C., Carolan, J. C., Coffey, M., & Kavanagh, K. (2018). Quantitative proteomics reveals divergent responses in *Apis mellifera* worker and drone pupae to parasitization by *Varroa destructor*. *Journal of Insect Physiology*, *107*, 291–301. https://doi.org/10.1016/j.jinsphys.2017.12.004
53. de Miranda, J. R., & Genersch, E. (2010). Deformed wing virus. *Journal of Invertebrate Pathology*, *103*(Supplement 1), S48–S61. https://doi.org/10.1016/j.jip.2009.06.012
54. Paxton, R. J., Schafer, M. O., Nazzi, F., Zanni, V., Annoscia, D., Marroni, F., Bigot, D., Laws-Quinn, E. R., Panziera, D., Jenkins, C., & Shafiey, H. (2022). Epidemiology of a major honey bee pathogen, deformed wing virus: Potential worldwide replacement of genotype A by genotype B. *International Journal for Parasitology: Parasites and Wildlife*, *18*, 157–171. https://doi.org/10.1016/j.ijppaw.2022.04.013
55. Foster, L. J. (2011). Interpretation of data underlying the link between colony collapse disorder (CCD) and an invertebrate iridescent virus. *Molecular & Cellular Proteomics*, *10*(3), M110006387. https://doi.org/10.1074/mcp.M110.006387
56. Morita, M., & Imanaka, T. (2019). The function of the peroxisome. In: T. Imanaka,& N. Shimozawa (Eds.), *Peroxisomes: biogenesis, function, and role in human disease* (pp. 59–104). Singapore: Springer. https://doi.org/10.1007/978-981-15-1169-1_4
57. Pridie, C., Ueda, K., & Simmonds, A. J. (2020). Rosy beginnings: Studying peroxisomes in *Drosophila*. *Frontiers in Cell and Developmental Biology*, *8*, 835. https://doi.org/10.3389/fcell.2020.00835
58. Tripathi, D. N., & Walker, C. L. (2016). The peroxisome as a cell signaling organelle. *Current Opinion in Cell Biology*, *39*, 109–112. https://doi.org/10.1016/j.ceb.2016.02.017
59. Sargsyan, Y., & Thoms, S. (2020). Staying in healthy contact: How peroxisomes interact with other cell organelles. *Trends in Molecular Medicine*, *26*(2), 201–214. https://doi.org/10.1016/j.molmed.2019.09.012
60. Schrader, M., Kamoshita, M., & Islinger, M. (2020). Organelle interplay—peroxisome interactions in health and disease. *Journal of Inherited Metabolic Disease*, *43*(1), 71–89. https://doi.org/10.1002/jimd.12083
61. Ivashchenko, O., Van Veldhoven, P. P., Brees, C., Ho, Y. E.-S., Terlecky, S. R., & Fransen, M. (2011). Intraperoxisomal redox balance in mammalian cells: Oxidative stress and interorganellar cross-talk. *Molecular Biology of the Cell*, *22*(9), 1440–1451. https://doi.org/10.1091/mbc.E10-11-0919
62. Knoops, B., Argyropoulou, V., Becker, S., Ferte, L., & Kuznetsova, O. (2016). Multiple roles of peroxiredoxins in inflammation. *Molecules and Cells*, *39*(1), 60–64. https://doi.org/10.14348/molcells.2016.2341
63. Radyuk, S. N., Michalak, K., Klichko, V. I., Benes, J., & Orr, W. C. (2010). Peroxiredoxin 5 modulates immune response in *Drosophila*. *Biochimica et Biophysica Acta (BBA)—General Subjects*, *1800*(11), 1153–1163. https://doi.org/10.1016/j.bbagen.2010.06.010

64. Shin, J. A., Chung, J. S., Cho, S.-H., Kim, H. J., & Yoo, Y. D. (2013). Romo1 expression contributes to oxidative stress-induced death of lung epithelial cells. *Biochemical and Biophysical Research Communications*, *439*(2), 315–320. https://doi.org/10.1016/j.bbrc.2013.07.012
65. Amini, M. A., Karimi, J., Talebi, S. S., & Piri, H. (2022). The association of COVID-19 and reactive oxygen species modulator 1 (ROMO1) with oxidative stress. *Chonnam Medical Journal*, *58*(1), 1–5. https://doi.org/10.4068/cmj.2022.58.1.1
66. Olejnik, J., Hume, A. J., & Muhlberger, E. (2018). Toll-like receptor 4 in acute viral infection: Too much of a good thing. *PLOS Pathogens*, *14*(12), e1007390. https://doi.org/10.1371/journal.ppat.1007390
67. Liaunardy-Jopeace, A., Bryant, C. E., & Gay, N. J. (2014). The COP II adaptor protein TMED7 is required to initiate and mediate the delivery of TLR4 to the plasma membrane. *Science Signaling*, *7*(336), ra70. https://doi.org/10.1126/scisignal.2005275
68. Saraya, R., Veenhuis, M., & van der Klei, I. J. (2010). Peroxisomes as dynamic organelles: Peroxisome abundance in yeast. *The FEBS Journal*, *277*(16), 3279–3288. https://doi.org/10.1111/j.1742-4658.2010.07740.x
69. Lippai, M., & Low, P. (2014). The role of the selective adaptor p62 and ubiquitin-like proteins in autophagy. *BioMed Research International*, *2014*, 832704. https://doi.org/10.1155/2014/832704
70. Bar-Peled, L., Schweitzer, L. D., Zoncu, R., & Sabatini, D. M. (2012). Ragulator is a GEF for the Rag GTPases that signal amino acid levels to mTORC1. *Cell*, *150*(6), 1196–1208. https://doi.org/10.1016/j.cell.2012.07.032
71. Sancak, Y., Bar-Peled, L., Zoncu, R., Markhard, A. L., Nada, S., & Sabatini, D. M. (2010). Ragulator-Rag complex targets mTORC1 to the lysosomal surface and is necessary for its activation by amino acids. *Cell*, *141*(2), 290–303. https://doi.org/10.1016/j.cell.2010.02.024
72. Eun, S. Y., Lee, J. N., Nam, I.-K., Liu, Z.-q., So, H.-S., Choe, S.-K., & Park, R. K. (2018). PEX5 regulates autophagy via the mTORC1-TFEB axis during starvation. *Experimental & Molecular Medicine*, *50*(4), 1–12. https://doi.org/10.1038/s12276-017-0007-8
73. Eid, W., Dauner, K., Courtney, K. C., Gagnon, A., Parks, R. J., Sorisky, A., & Zha, X. (2017). mTORC1 activates SREBP-2 by suppressing cholesterol trafficking to lysosomes in mammalian cells. *Proceedings of the National Academy of Sciences of the United States of America*, *114*(30), 7999–8004. https://doi.org/10.1073/pnas.1705304114
74. Glitscher, M., & Hildt, E. (2021). Endosomal cholesterol in viral infections—a common denominator? *Frontiers in Physiology*, *12*, 750544. https://doi.org/10.3389/fphys.2021.750544
75. Li, N. A., Hua, B., Chen, Q., Teng, F., Ruan, M., Zhu, M., Zhang, L. I., Huo, Y., Liu, H., Zhuang, M., Shen, H., & Zhu, H. (2022). A sphingolipid-mTORC1 nutrient-sensing pathway regulates animal development by an intestinal peroxisome relocation-based gut-brain crosstalk. *Cell Reports*, *40*(4), 111140. https://doi.org/10.1016/j.celrep.2022.111140
76. Wang, X., Beugnet, A., Murakami, M., Yamanaka, S., & Proud, C. G. (2005). Distinct signaling events downstream of mTOR cooperate to mediate the effects of amino acids and insulin on initiation factor 4E-binding proteins. *Molecular and Cellular Biology*, *25*(7), 2558–2572. https://doi.org/10.1128/MCB.25.7.2558-2572.2005
77. Thedieck, K., & Hall, M. N. (2010). Translational control by amino acids and energy. In: R. A. Bradshaw, & E. A. Dennis (Eds.), *Handbook of cell signaling*, Vol. 3, 2nd edn. (pp. 2285–2293). Amsterdam: Elsevier/Academic Press. https://doi.org/10.1016/B978-0-12-374145-5.00274-6
78. Gingras, A.-C., Gygi, S. P., Raught, B., Polakiewicz, R. D., Abraham, R. T., Hoekstra, M. F., Aebersold, R., & Sonenberg, N. (1999). Regulation of 4E-BP1 phosphorylation: a novel two-step mechanism. *Genes & Development*, *13*(11), 1422–1437. https://doi.org/10.1101/gad.13.11.1422
79. Karaki, S., Andrieu, C., Ziouziou, H., & Rocchi, P. (2015). The eukaryotic translation initiation factor 4E (eIF4E) as a therapeutic target for cancer. *Advances in Protein Chemistry and Structural Biology*, *101*, 1–26. https://doi.org/10.1016/bs.apcsb.2015.09.001
80. Perez-Gil, G., Landa-Cardena, A., Coutino, R., Garcia-Roman, R., Sampieri, C. L., Mora, S. I., & Montero, H. (2015). 4EBP1 is dephosphorylated by respiratory syncytial virus infection. *Intervirology*, *58*(4), 205–208. https://doi.org/10.1159/000435774
81. Connor, J. H., & Lyles, D. S. (2002). Vesicular stomatitis virus infection alters the eIF4F translation initiation complex and causes dephosphorylation of the eIF4E binding protein 4E-BP1. *Journal of Virology*, *76*(20), 10177–10187. https://doi.org/10.1128/jvi.76.20.10177-10187.2002
82. Stern-Ginossar, N., Thompson, S. R., Mathews, M. B., & Mohr, I. (2019). Translational control in virus-infected cells. *Cold Spring Harbor Perspectives in Biology*, *11*(3), a033001. https://doi.org/10.1101/cshperspect.a033001
83. Woodcock, H. V., Eley, J. D., Guillotin, D., Plate, M., Nanthakumar, C. B., Martufi, M., Peace, S., Joberty, G., Poeckel, D., Good, R. B., Taylor, A. R., Zinn, N., Redding, M., Forty, E. J., Hynds, R. E., Swanton, C., Karsdal, M., Maher, T. M., Fisher, A., … Chambers, R. C. (2019). The mTORC1/4E-BP1 axis represents a critical signaling node during fibrogenesis. *Nature Communications*, *10*(1), 6. https://doi.org/10.1038/s41467-018-07858-8
84. Kisseleva, T., & Brenner, D. A. (2008). Mechanisms of fibrogenesis. *Experimental Biology and Medicine*, *233*(2), 109–122. https://doi.org/10.3181/0707-MR-190
85. Wang, J., Cui, B., Chen, Z., & Ding, X. (2022). The regulation of skin homeostasis, repair and the pathogenesis of skin diseases by spatiotemporal activation of epidermal mTOR signaling. *Frontiers in Cell and Developmental Biology*, *10*, 950973. https://doi.org/10.3389/fcell.2022.950973
86. Mihaylova, M. M., & Shaw, R. J. (2011). The AMPK signalling pathway coordinates cell growth, autophagy and metabolism. *Nature Cell Biology*, *13*(9), 1016–1023. https://doi.org/10.1038/ncb2329
87. Chaudhury, A., & Howe, P. H. (2009). The tale of transforming growth factor-beta (TGFβ) signaling: A soigne enigma. *IUBMB Life*, *61*(10), 929–939. https://doi.org/10.1002/iub.239
88. Ramirez, H., Patel, S. B., & Pastar, I. (2014). The role of TGFβ signaling in wound epithelialization. *Advances in Wound Care*, *3*(7), 482–491. https://doi.org/10.1089/wound.2013.0466
89. Sanjabi, S., Oh, S. A., & Li, M. O. (2017). Regulation of the immune response by TGF-β: From conception to autoimmunity and infection. *Cold Spring Harbor Perspectives in Biology*, *9*(6), a022236. https://doi.org/10.1101/cshperspect.a022236
90. Upadhyay, A., Moss-Taylor, L., Kim, M.-J., Ghosh, A. C., & O'Connor, M. B. (2017). TGF-β family signaling in drosophila. *Cold Spring Harbor Perspectives in Biology*, *9*(9), a022152. https://doi.org/10.1101/cshperspect.a022152
91. Lamouille, S., & Derynck, R. (2007). Cell size and invasion in TGF-β–induced epithelial to mesenchymal transition is regulated by activation of the mTOR pathway. *Journal of Cell Biology*, *178*(3), 437–451. https://doi.org/10.1083/jcb.200611146
92. Honda, D., Okumura, M., & Chihara, T. (2023). Crosstalk between the mTOR and Hippo pathways. *Development, Growth & Differentiation*, *65*(6), 337–347. https://doi.org/10.1111/dgd.12867
93. Zhang, S., Liang, S., Wu, D., Guo, H., Ma, K., & Liu, L. (2021). LncRNA coordinates Hippo and mTORC1 pathway activation in cancer. *Cell Death & Disease*, *12*(9), 822. https://doi.org/10.1038/s41419-021-04112-w
94. Kulaberoglu, Y., Lin, K., Holder, M., Gai, Z., Gomez, M., Assefa Shifa, B., Mavis, M., Hoa, L., Sharif, A. A. D., Lujan, C., Smith, E. S. J., Bjedov, I., Tapon, N., Wu, G., & Hergovich, A. (2017). Stable MOB1 interaction with Hippo/MST is not essential for development and tissue growth

control. *Nature Communications*, *8*(1), 695. https://doi.org/10.1038/s41467-017-00795-y
95. Liu, B. O., Zheng, Y., Yin, F., Yu, J., Silverman, N., & Pan, D. (2016). Toll receptor-mediated Hippo signaling controls innate immunity in *Drosophila*. *Cell*, *164*(3), 406–419. https://doi.org/10.1016/j.cell.2015.12.029
96. Huang, Y., Ma, F.-t., & Ren, Q. (2020). Function of the MOB kinase activator-like 1 in the innate immune defense of the oriental river prawn (*Macrobrachium nipponense*). *Fish & Shellfish Immunology*, *102*, 440–448.
97. Munoz-Wolf, N., & Lavelle, E. C. (2017). Hippo interferes with antiviral defences. *Nature Cell Biology*, *19*(4), 267–269. https://doi.org/10.1038/ncb3502
98. Wang, Z., Lu, W., Zhang, Y., Zou, F., Jin, Z., & Zhao, T. (2020). The Hippo pathway and viral infections. *Frontiers in Microbiology*, *10*, 3033. https://doi.org/10.3389/fmicb.2019.03033
99. Weaver, D. B., Cantarel, B. L., Elsik, C. G., Boncristiani, D. L., & Evans, J. D. (2021). Multi-tiered analyses of honey bees that resist or succumb to parasitic mites and viruses. *BMC Genomics*, *22*(1), 720. https://doi.org/10.1186/s12864-021-08032-z
100. Yu, F.-X., & Guan, K.-L. (2013). The Hippo pathway: Regulators and regulations. *Genes & Development*, *27*(4), 355–371. https://doi.org/10.1101/gad.210773.112
101. Dutta, S., Mana-Capelli, S., Paramasivam, M., Dasgupta, I., Cirka, H., Billiar, K., & Mccollum, D. (2018). TRIP6 inhibits Hippo signaling in response to tension at adherens junctions. *EMBO Reports*, *19*(2), 337–350. https://doi.org/10.15252/embr.201744777
102. Lin, V. T. G., & Lin, F.-T. (2011). TRIP6: An adaptor protein that regulates cell motility, antiapoptotic signaling and transcriptional activity. *Cellular Signalling*, *23*(11), 1691–1697. https://doi.org/10.1016/j.cellsig.2011.06.004
103. Karpova, N., Bobinnec, Y., Fouix, S., Huitorel, P., & Debec, A. (2006). Jupiter, a new *Drosophila* protein associated with microtubules. *Cell Motility and the Cytoskeleton*, *63*(5), 301–312. https://doi.org/10.1002/cm.20124
104. Martinez, D., Zhu, M., Guidry, J. J., Majeste, N., Mao, H., Yanofsky, S. T., Tian, X., & Wu, C. (2021). Mask, the *Drosophila* ankyrin repeat and KH domain-containing protein, affects microtubule stability. *Journal of Cell Science*, *134*(20), jcs258512. https://doi.org/10.1242/jcs.258512
105. Walsh, D., & Naghavi, M. H. (2019). Exploitation of cytoskeletal networks during early viral infection. *Trends in Microbiology*, *27*(1), 39–50. https://doi.org/10.1016/j.tim.2018.06.008
106. Marsh, M. (2005). *Membrane trafficking in viral replication*. Berlin, Heidelberg: Springer. https://doi.org/10.1007/b138037
107. Hernandez-Gonzalez, M., Larocque, G., & Way, M. (2021). Viral use and subversion of membrane organization and trafficking. *Journal of Cell Science*, *134*(5), jcs252676. https://doi.org/10.1242/jcs.25267
108. Taylor, M. P., Koyuncu, O. O., & Enquist, L. W. (2011). Subversion of the actin cytoskeleton during viral infection. *Nature Reviews Microbiology*, *9*(6), 427–439. https://doi.org/10.1038/nrmicro2574
109. Seo, D., & Gammon, D. B. (2022). Manipulation of host microtubule networks by viral microtubule-associated proteins. *Viruses*, *14*(5), 979. https://doi.org/10.3390/v14050979
110. Badaoui, B., Fougeroux, A., Petit, F., Anselmo, A., Gorni, C., Cucurachi, M., Cersini, A., Granato, A., Cardeti, G., Formato, G., Mutinelli, F., Giuffra, E., Williams, J. L., & Botti, S. (2017). RNA-sequence analysis of gene expression from honeybees (*Apis mellifera*) infected with *Nosema ceranae*. *PLOS ONE*, *12*(3), e0173438. https://doi.org/10.1371/journal.pone.0173438
111. Kanbar, G., & Engels, W. (2004). Visualisation by vital staining with trypan blue of wounds punctured by *Varroa destructor* mites in pupae of the honey bee (*Apis mellifera*). *Apidologie*, *35*(1), 25–29. https://doi.org/10.1051/apido:2003057
112. Parker, R., Guarna, M. M., Melathopoulos, A. P., Moon, K.-M., White, R., Huxter, E., Pernal, S. F., & Foster, L. J. (2012). Correlation of proteome-wide changes with social immunity behaviors provides insight into resistance to the parasitic mite, *Varroa destructor*, in the honey bee (*Apis mellifera*). *Genome Biology*, *13*(9), R81. https://doi.org/10.1186/gb-2012-13-9-r81
113. Li, J., Ma, L., Lin, Z., Zou, Z., & Lu, Z. (2016). Serpin-5 regulates prophenoloxidase activation and antimicrobial peptide pathways in the silkworm, *Bombyx mori*. *Insect Biochemistry and Molecular Biology*, *73*, 27–37. https://doi.org/10.1016/j.ibmb.2016.04.003
114. An, C., & Kanost, M. R. (2010). *Manduca sexta* serpin-5 regulates prophenoloxidase activation and the Toll signaling pathway by inhibiting hemolymph proteinase HP6. *Insect Biochemistry and Molecular Biology*, *40*(9), 683–689. https://doi.org/10.1016/j.ibmb.2010.07.001
115. Katsukawa, M., Ohsawa, S., Zhang, L., Yan, Y., & Igaki, T. (2018). Serpin facilitates tumor-suppressive cell competition by blocking Toll-mediated Yki activation in *Drosophila*. *Current Biology*, *28*(11), 1756–1767.e6.e1756. https://doi.org/10.1016/j.cub.2018.04.022

SUPPORTING INFORMATION

Additional supporting information may be found online https://doi.org/10.1002/pmic.202300312 in the Supporting Information section at the end of the article.

How to cite this article: Erban, T., Kadleckova, D., Sopko, B., Harant, K., Talacko, P., Markovic, M., Salakova, M., Kadlikova, K., Tachezy, R., & Tachezy, J. (2024). *Varroa* destructor parasitism and Deformed wing virus infection in honey bees are linked to peroxisome-induced pathways. *Proteomics*, *24*, e2300312. https://doi.org/10.1002/pmic.202300312